Structure of an Evolving Hailstorm, Part V: Synthesis and Implications for Hail Growth and Hail Suppression

K. A. Browning[1], J. C. Fankhauser, J.-P. Chalon[2] and P. J. Eccles

National Center for Atmospheric Research,[3] Boulder, Colo. 80303

R. G. Strauch and F. H. Merrem

NOAA/ERL/Wave Propagation Laboratory, Boulder, Colo. 80303

D. J. Musil, E. L. May and W. R. Sand

Institute of Atmospheric Sciences, South Dakota School of Mines and Technology, Rapid City, S. Dak. 57701

(Manuscript received 17 September 1975, in revised form 6 January 1976)

ABSTRACT

A model of an evolving hailstorm is synthesized from data presented in four related papers in this issue. The storm model, which is applicable to a class of ordinary multicell hailstorms and similar to earlier models derived by workers in South Dakota and Alberta, is discussed in terms of the growth of hail and its implications for hail suppression. Hail is grown in time-evolving updrafts that begin as discrete new clouds on the flank of the storm. Low concentrations of embryos develop rapidly within each of these clouds. The embryos subsequently grow into small hailstones while suspended near or above the −20°C level as each new cloud grows and becomes the main updraft. Recycling is not a feature of this model as it is in supercell models. To improve the chance of silver iodide seeding being effective in suppressing the growth of hail in multicell storms, it is proposed that the seeding should be carried out not in the main updraft as is often the practice, but, rather, in the regions of weaker updraft associated with the early stages of developing clouds on the flank of the storm.

1. Introduction: the ordinary multicell storm as a distinct hailstorm type

Several categories of hailstorms have recently been proposed (Marwitz, 1972 a, b, c; Chisholm and Renick, 1972). According to Browning (1975), one of the most important distinctions is between ordinary multicell storms and supercell storms. The essential difference between these two types is that, whereas a supercell storm is dominated by a single cell which attains a quasi-steady structure with updrafts and downdrafts coexisting symbiotically for long periods, an ordinary multicell storm consists of a sequence of evolving cells each of which may go through a life-cycle resembling that first described in the Thunderstorm Project (Byers and Braham, 1949). Both kinds of storms can produce damaging hail and, although the biggest and most damaging hailstorms tend to be supercells, the majority of hailstorms in the North American continent appear to be of the ordinary multicell variety.

Each new updraft cell in an ordinary multicell storm is seen first as a discrete new growing cumulus cloud. During Project Hailswath (Goyer *et al.*, 1966) these became known as feeder clouds. This term can be misleading when applied to ordinary multicell storms in the sense that the clouds do not *feed* the mature hail cloud but, rather, grow and *become* the mature hail cloud. Therefore, we refer to them instead as daughter clouds. Such clouds have been discussed by Dennis *et al.* (1970) and Musil (1970). They consider them to be one of the most striking visual phenomena associated with Great Plains thunderstorms. They find that the daughter clouds begin forming at distances up to 30 km away from the hailstorm core. Each cloud grows rapidly as it approaches and merges with the main cumulonimbus cloud mass. For an eastward-moving storm the merger usually takes place on the southwestern side of the main cloud mass and occurs 15–40 min after the initial formation of the daughter cloud. As shown in Fig. 1, a first radar echo usually appears in a daughter cloud just before it merges fully with the main cloud mass. A burst of heavy rain or hail usually reaches the ground soon after the merger. The evolution of the individual areas of heavier precipitation associated with

[1] On leave from the Meteorological Office Research Unit, Royal Radar Establishment, Malvern, England.

[2] On leave from Météorologie Nationale, France, on a fellowship from the Délégation Générale à la Recherche Scientifique et Technique.

[3] This research was performed as part of the National Hail Research Experiment, managed by the National Center for Atmospheric Research and sponsored by the Weather Modification Program, Research Applications Directorate, National Science Foundation.

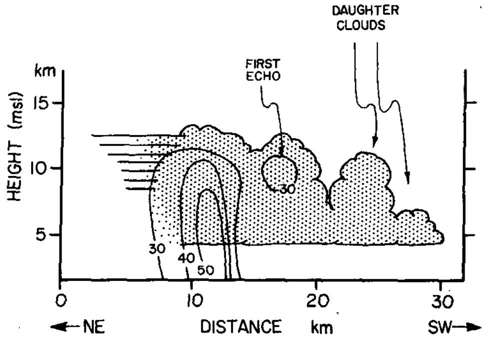

FIG. 1. Schematic diagram showing an NE-SW cross section through a typical hailstorm of western South Dakota. Stippled shading denotes cloud; solid contours represent radar reflectivity in dBz (adapted from Dennis *et al.*, 1970).

successive cells has been studied by Renick (1971). He shows that the individual cells may produce hail for periods of up to 30 min. At the surface this gives rise to families of what Changnon (1970) refers to as hail-streaks. Since the new cells usually form on the right flank, the storm as a whole propagates discretely to the right of the cell motion (Browning, 1962; Renick, 1971; Marwitz, 1972b).

The purpose of this paper is to present a model of the storm that gave hail in the vicinity of Raymer, Colorado, on 9 July 1973, synthesized from data in Parts I through IV. As we shall show, the model conforms in many ways to the above description of ordinary multicell storms. Of course, this is not to say that all such storms can be expected to fit this model. The maximum temperature excess in the updraft, assuming unmixed parcel ascent, was 5°C; the mean wind shear in the layer from cloud base to cloud top (650–150 mb) was about 2×10^{-3} s^{-1}; and the mean wind in the subcloud layer was 8 m s^{-1}. According to Marwitz (1972b) these values are characteristic of the environment of multicell hailstorms. In terms of the updraft intensity, the frequency of development of new cells and the resulting hail size, the Raymer hailstorm can be categorized as being of moderate intensity.

2. Model of the Raymer hailstorm

Figures 2 and 3 are simplified representations of the Raymer storm, each depicting a vertical section along the storm's direction of travel (approximately north to south). The former figure is highly schematic; the latter is rather more realistic.

Figure 2 shows the configuration of the updraft circulation derived from the observations, and also the way it depends on the environmental winds. The wind pattern was rather complex but the main feature distilled here is that the storm traveled roughly with the winds in the middle troposphere, the winds in the lower and upper troposphere having a component from south to north relative to the storm. As in the case of some low-latitude storms (e.g., Ludlam, 1963; Zipser, 1969), this caused air to feed the updraft from the front of the storm and to leave it as an anvil trailing to the rear. Owing to strong veer of the environmental winds with height relative to the storm, the inflow actually approached the updraft with a small component also from beneath the page in Fig. 2 and the anvil outflow left with a strong component back into the page. However, because of the general rearward tilt of the updraft most of the small hailstones which grew within the updraft probably descended directly into the underlying downdraft rather than re-entering the updraft. Thus, although turbulent motions may have transferred some particles from an older updraft cell to a younger one, the majority of particles would probably have been denied the chance of a second ascent in which to continue their growth into larger stones. A similar (although steadier) updraft configuration to that in Fig. 2 has been inferred for a supercell storm by Browning and Foote (1976) but in that case strong winds blowing around the storm in the middle troposphere were able to carry particles around the periphery of the updraft so that they could indeed re-enter the foot of the updraft.

Figure 3 (top) embellishes the model with more detailed information from Parts I–IV. Plotted at the bottom of the figure are curves showing the variation of updraft velocity and water content along the line NS at a height of 7.2 km (all heights are above MSL). Different parts of Fig. 3 were derived from different sources of data obtained over a period of about an hour during which a sequence of five cells was observed. Times and sources of the data are plotted in Table 1.

The model in Fig. 3 can be interpreted in two ways. It can either be regarded as an instantaneous view of a typical structure with four different cells at different stages of evolution or it can be regarded as showing four stages in the evolution of an individual cell. Thus Cell n, which had developed a "first echo" shortly before the time portrayed in Fig. 3, began growing out of the shelf cloud as a distinct daughter cloud ($n+1$)

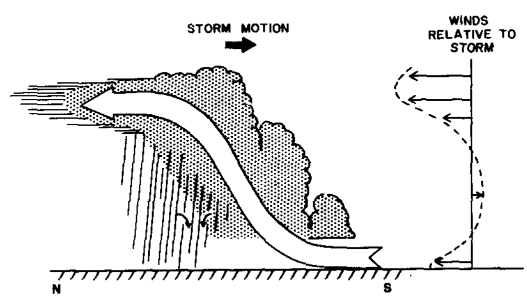

FIG. 2. Schematic diagram showing the configuration of the updraft in the Raymer hailstorm in relation to the environmental flow. (Strictly the updraft was in the form of a chain of contiguous updraft elements with centers lying along the arrow shown in the figure.)

about 15 min earlier. Cell $n-1$, which has almost reached its maximum reflectivity, is in its mature stage; it has a vigorous updraft but part of it has been converted into a vigorous downdraft. The decaying Cell $n-2$ is characterized by weak downdrafts at most levels, with a residual weak updraft in places aloft. The

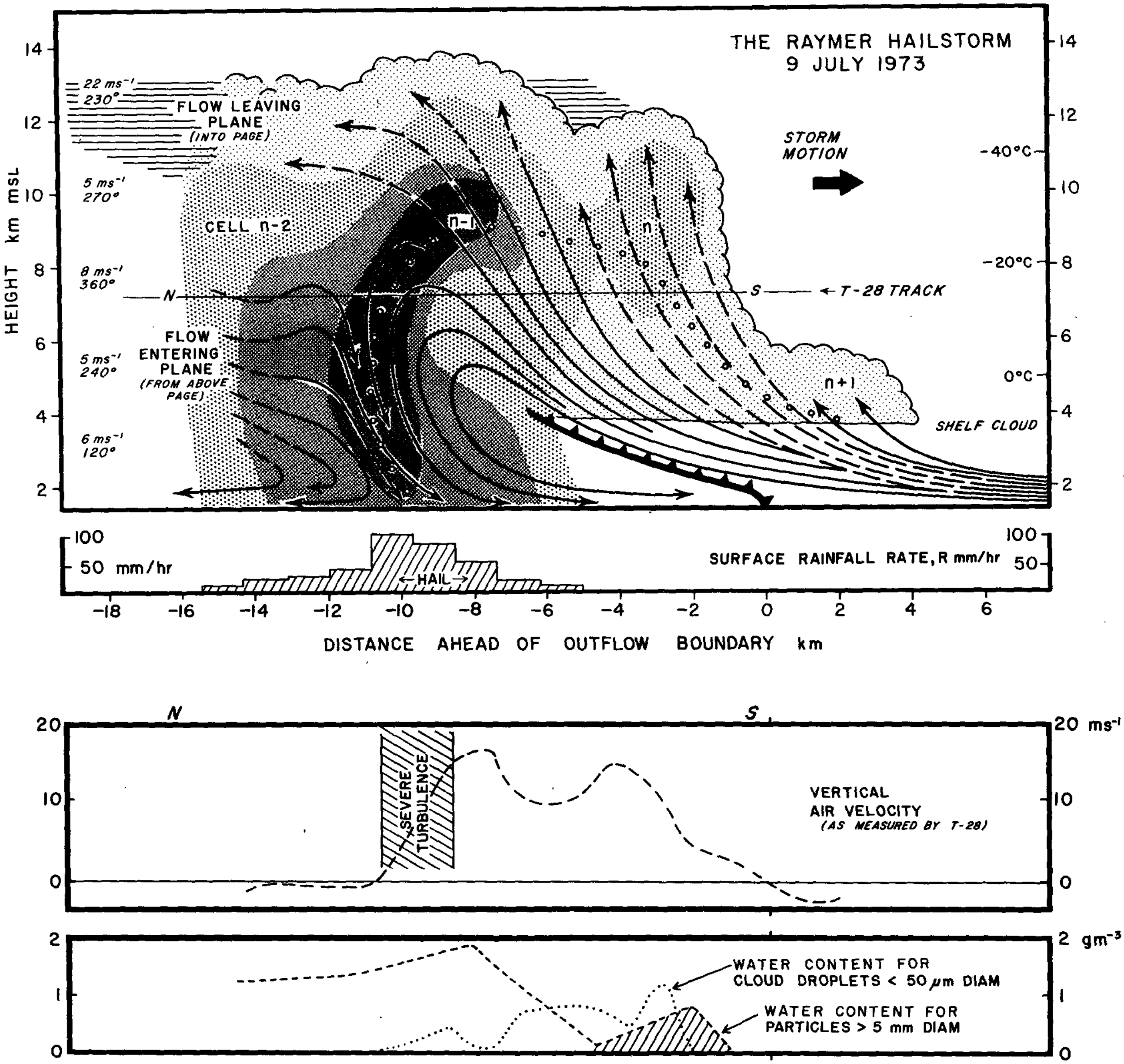

FIG. 3. Schematic model (top) of the Raymer hailstorm showing a vertical section along the storm's direction of travel through a sequence of evolving cells. Solid lines are streamlines of flow relative to the moving system; they are shown broken on the left side of the figure to represent flow into and out of the plane and on the right side of the figure to represent flow remaining within a plane a few kilometers closer to the reader. The open circles represent the trajectory of a hailstone during its growth from a small droplet at cloud base (see text). (Actually the airflow in each cell has been drawn relative to the individual cell and, since the developing Cells $n+1$ and n traveled more slowly (5 m s^{-1}) than either the mature cells (7 m s^{-1}) or the storm as a whole (10 m s^{-1}), the streamlines in the young cells would have had a stronger component from the south relative to the storm as a whole. This explains why in the model the trajectory of the growing hailstone crosses over the streamlines during its early growth as shown in the figure.) Lightly stippled shading represents the extent of cloud and the three darker grades of stippled shading represent radar reflectivities of 35, 45, and 50 dBz. The temperature scale on the right side represents the temperature of a parcel lifted from the surface. Winds (m s^{-1}, deg) on the left side are environmental winds relative to the storm based on soundings behind the storm. Surface rainfall rate averaged over 2 min intervals during the passage of the storm is plotted below the section. The horizontal line NS through the section at 7.2 km shows the track of the T-28 penetration aircraft, smoothed data from which are plotted at the foot of the figure. Although the T-28 data were not quite synchronous with the data in the vertical section, a comparison of the T-28 updraft velocity measurements with the flow pattern in the vertical section shows that the agreement is reasonably good.

TABLE 1. Times and sources of data in Fig. 3.

Data	Source	Time (MDT)
Radar echo	Grover 10 cm radar (See Part I)	1716–1717
Visual cloud	Airborne photographs (Part II)	1719
Inflow to updraft and gust front	4 aircraft at sub-cloud levels (Part II)	1642–1727
	Surface mesometeorological network (Part II)	1655–1727
Airflow within interior of storm	2 Doppler radars (Part III)	1727–1736
Microphysical measurements in relation to vertical air motion	T-28 penetration aircraft (Part IV)	1717–1720

time interval between development of successive cells was 15±2 min; it took 15 min for n to evolve to the stage of development of $n-1$, and similarly for $n-1$ to evolve to $n-2$. The total lifetime of each cell was about 45 min. The lifetime for individual radar echoes was rather longer than the average figure for singlecell echoes reported by Battan (1953).

The entire inflow toward the updraft originated close to the ground ahead of the storm; at a distance of 20 km upwind of the updraft the inflow was about 500 m deep. The inflow rose unmixed to cloud base, consistent with the laminar flow generally observed below cloud base in earlier studies (e.g., Auer *et al.*, 1970). The lateral dimensions of individual updraft cells, about 8 km at cloud base level, are similar to the average value for High Plains hailstorms found by Auer and Marwitz (1968). Cell dimensions decreased in the present case to roughly 5 km in the middle troposphere. Successive updraft cells may have been separated by an area of weak subsidence at cloud base level but they were contiguous at higher levels, giving rise to a fairly broad region of general updraft aloft. The *maximum* updraft velocity in a mature cell reached 6 to 8 m s^{-1} at cloud base and 20 m s^{-1} at 7 km MSL just above the level of maximum parcel buoyancy. The *average* value of the updraft at cloud base was 4 m s^{-1}, again similar to that measured by Auer and Marwitz (1968) in typical High Plains hailstorms. Horizontal momentum was conserved in parts of the updraft, the relative southerly component being 10 to 12 m s^{-1} in the inflow below cloud base and also in the updraft core at 7 km, but decreasing by a few meters per second in the core at 10 km. The outflow from the updraft formed an anvil which was directed mainly toward the left rear flank of the storm (to the left and into the page). The entire updraft was tilted toward the rear of the storm and, as noted above, there seemed to be little opportunity for precipitation particles grown within one cell to be recycled into a younger cell.

As for the downdraft, part of it originated in the midtroposphere at the level of lowest equivalent potential temperature (6 km) and descended unmixed to the surface; this air entered the storm on its right rear flank (from the left of and above the page). Some of the downdraft was also probably generated within former updraft air. This is suggested by the form of the streamlines in Fig. 3 but the possibility of motion out of the plane weakens the inference somewhat. The maximum observed downdraft velocity of 15 m s^{-1} was located in the region of highest radar reflectivity, close to cloud base level. Downdraft velocities greater than 10 m s^{-1} occurred in a region 2 km wide extending from a height of 2 to 6 km. A pronounced maximum of turbulence intensity existed at the updraft-downdraft interface of the mature cell; it reached a peak near the level of maximum parcel buoyancy (7 km). The depth of the surface outflow exceeded 1 km ahead of the storm, but behind the storm the depth of downdraft air that was directed rearward relative to the storm was less than 500 m. Surface divergence beneath the strongest downdraft was 4×10^{-3} s^{-1}. Maximum surface convergence at the inflow-outflow interface was 1 to 2×10^{-3} s^{-1}. On average the gust front extended 5 km ahead of the leading edge of the surface precipitation, a feature which according to Auer *et al.* (1969) is typical of intense and persistent hailstorms.

Measurements with the penetration aircraft indicated that supercooled water was most abundant in the young updraft regions in the vicinity of the "first echo." Small supercooled droplets (diameter <50 μm) were present at the 7 km level in amounts of about 1 g m^{-3}. This is about a third of the adiabatic content. The "first echo" in each cell occurred typically at -12°C (7 km MSL), rather lower than usual for High Plains hailstorms (Browning, 1975). Shortly after the appearance of the first echo it contained particles 5 mm in diameter in a number concentration of 1 m^{-3}; most of these larger particles were frozen but a few (up to 25%) appeared to be entirely water. The mature cell ($n-1$) contained particles with diameter 8 to 10 mm in concentrations of about 0.5 m^{-3} at a height of 7 km. These particles, which accounted for most of the maximum radar reflectivity, were almost entirely of ice and were most abundant on the rear edge of the updraft and in the downdraft. Large concentrations of water corresponding to possible "accumulation zones" (Sulakvelidze *et al.*, 1967) were not found. Heavy rain (~100 mm h^{-1}) and hail (maximum diameter 15 mm) reached the surface, giving a total of 12 mm in 20 min of which 5% was due to hail. Although no hail was collected for the particular storm of interest, in a nearby storm 25% of the hailstone embryos were frozen drops and 75% were graupel.

3. Growth of hail in the Raymer storm

In the previous section we summarized the bare facts about the storm structure as derived in Parts I to IV. We now attempt to piece some of these facts together in a more speculative way to infer the likely growth conditions for the hail and also the possible influence of silver iodide seeding.

Large hailstones have fallspeeds V_t of 20 m s^{-1} or more and in any theory their production requires that the updraft in which they are grown shall have comparable speeds. However, in the early stages of its growth (when $V_t < 10$ m s^{-1}) the fallspeed of a hailstone embryo increases rather slowly and a steady strong updraft would carry it through the supercooled zone of a cloud before it could attain a large size (Ludlam, 1958). A favorable growth regime can occur in at least two ways. One way is for an embryo to grow during an ascent on the edge of a quasi-steady updraft where the vertical velocity is relatively weak and then, after its terminal fallspeed has reached about 10 m s^{-1}, for it to get carried around to the inflow side of the main updraft to enter the core of the updraft at a low level. Such a behavior probably applies to supercell storms (Browning and Foote, 1976) but is not applicable to the Raymer storm because individual updraft cells were short-lived and in any case there were no significant components of flow aloft capable of causing the embryos to recycle in this way; neither does it seem likely that turbulence can have transferred many such particles from the mature cells into the daughter clouds against the mean flow. A second way for the embryos to grow, exemplified in this case study, is for them to grow in a time-developing updraft. The young daughter clouds which characterize an ordinary multicell storm are thus favored regions for the growth of embryos because they do not develop into strong updrafts until some time after the initial cloud formation (Musil, 1970).

In the Raymer storm the early growth of embryos typically 5 mm in diameter from small cloud particles seems likely to have occurred within newly rising daughter clouds going from the $n+1$ position in Fig. 3 to the n position (see trajectory in Fig. 3). The subsequent motion of the embryos was determined by tracking local volumes of relatively high reflectivity through the storm echo (see Part I). This showed that the further growth of the embryos into hailstones which reached the ground 10 to 15 mm in diameter occurred while the particles (mean terminal fallspeed $\sim$20 m s^{-1}) were essentially balanced within the updraft as Cell n moved into the $n-1$ position in Fig. 3. Recall, now, that the flow pattern in Fig. 3 is drawn relative to each individual cell and that the developing cells were moving relatively at 5 m s^{-1} into the main storm system. During their growth most of the small hailstones probably will have remained within the same updraft cell as the cell moved through the storm system. In this case, the apparent crossing of the hail trajectory from one cell to another in Fig. 3 can be construed as a stone staying within a single cell as the cell goes through successive phases of development. On the other hand, hailstone embryos growing on the northern edge of Cell n may have descended into part of the older updraft associated with Cell $n-1$, just as the stones in the unsteady hailstorm observed by Battan (1975) sometimes appeared to be falling from one small updraft core into another. In either event the hailstones at this stage were evidently encountering updraft velocities sufficient to keep them aloft without major fluctuations in altitude.

The final stage in the hailstone growth history was for the particle content to increase to about 2 g m^{-3} near the region in Fig. 3 where the reflectivity exceeds 50 dBz. It appears that precipitation loading and, more importantly, mixing with low-θ_e air, began to have an effect here, for the lower portions of the updraft were quickly converted into a downdraft, and the hailstones cascaded rapidly to the ground with negligible further growth in a region almost depleted of supercooled water. Taking a mean terminal fallspeed of 23 m s^{-1} for hailstones 15 mm in diameter and a mean downdraft velocity of 10 m s^{-1}, such particles will have descended from 8 km to the ground at 1.5 km MSL in as little as 200 s. For a period of about 120 s the stones will have been descending below the 0°C level. As a result of melting such stones will have reached the ground about 13 mm in diameter (Ludlam, 1958).

Growth of the hailstones from embryos nominally 5 mm in diameter to stones 15 mm across is believed to have occurred as they were carried more or less horizontally relative to the storm system through a distance of 6 km at an ambient temperature between −20 and −30°C (Fig. 3). Taking a relative horizontal velocity of 8 m s^{-1}, consistent with the Doppler radar measurements in Part III, gives a period of 750 s. According to Ludlam (1958), this period is sufficient to account for growth from 5 to 15 mm diameter in the presence of a cloud water content of 1 g m^{-3}. This is broadly consistent with the values measured by the T-28.

The most difficult stage of growth to reconstruct is the development of the 5 mm embryos during the approximately 15 min period of initial growth of the daughter cloud. It has been suggested that the ice-crystal/graupel mechanism is the dominant process in High Plains storms (e.g., Dye *et al.*, 1974), and the fact that 75% of the embryos in a nearby storm on this occasion were graupel tends to support this view. However, there remains the problem of accounting for the remaining 25% of frozen-drop embryos in the nearby storm and the similar proportion of large all-water drops in the region of the first echo in the Raymer storm. We have already shown that the flow pattern in this storm was not conducive to such particles having been recycled from other, more mature, parts of the storm. Possibly these large drops did begin as graupel and experienced a brief turbulent excursion below the 0°C level during the growth of an individual daughter cloud. Alternatively the few large water drops encountered in the region of the first echo may have been due to growth by coalescence. As shown by Danielsen *et al.* (1972), for coalescence to account for the observed growth rate, it is necessary to assume the existence of rare large cloud droplets at cloud base. Perhaps these arose due to the presence of a few large aerosol particles; such particles have been detected within hailstones and are probably due to wind-raised dust (Rosinski, 1966; Rosinski and Kerrigan, 1969).

The above discussion indicates that the nature of the early growth is still open to question although the balance of evidence suggests that the ice crystal/graupel mechanism is likely to predominate. It is clearly important that more aircraft penetrations of daughter clouds (i.e., first echo regions) should be made, especially using instruments which are specially designed to identify the phase of the hydrometeors (e.g., Cannon, 1974). However, the uncertainties that exist should not detract from the general conclusions that (1) the embryos originate in the young daughter clouds, (2) they grow into hailstones while suspended at high levels after the updraft has become strong, and (3) they follow a trajectory broadly resembling that depicted in Fig. 3. These conclusions are similar to those reached by Musil (1970) and Renick (1971).

It is instructive to compare the vertical section in Fig. 3 with that through supercell storms—see e.g., Fig. 11 of Browning and Foote (1976). In both cases the updraft enters the storm within a weak echo region (WER). In the supercell the WER is in the form of a vault bounded by an overhanging curtain of echo containing embryos which have formed elsewhere and have circulated around the edge of the updraft so as to reenter it on its forward side. In the ordinary multicell storm the WER is not bounded: there are probably no recirculating embryos either. Instead the embryos form in situ during relatively weak ascent on the leading edge of the WER. In a supercell the re-entering embryos grow into hailstones while crossing over the vault from front to back; the newly-grown embryos in an ordinary multicell storm, on the other hand, grow into hailstones while they (and their associated first echo) are first suspended above and then descend into the WER. In a supercell the growth of the hailstones on the edge of the vault is favored since they are the first large particles to encounter undepleted cloud water in the updraft: to use the terminology of Browning and Foote (1976), they "compete unfairly" for the cloud water in the updraft. To some extent this may still be true of particles above the WER in an ordinary multicell storm as they descend into the WER. However, there is evidence that, whereas the updraft in a supercell is sufficiently strong and continuous both to prevent any cloud droplets attaining precipitation size within the vault and to prevent precipitation from entering it from its periphery, the same does not necessarily apply in the WER of an ordinary multicell storm. Perhaps because of rapid growth on very large aerosol particles or because of turbulence bringing in particles from the side, additional precipitation particles appear beneath the particles descending from the original first echo. They can be seen, for example, as the extensive region of relatively weak echo on the inflow side of the high reflectivity hailshaft in Fig. 3; in supercells this region is usually absent and there is instead an abrupt transition from no detectable echo in the vault to the high-reflectivity hailshaft bounding the vault. The presence of such particles, provided they are frozen, would have the effect of depleting the cloud water from which the original large embryos are able to grow and might account for the low cloud water content measured aloft by the T-28. These additional precipitation particles, being situated close to where the updraft is converted into a downdraft, are not themselves likely to grow into hail since they fall out of the updraft prematurely. Any effect of this kind would of course tend to suppress hail growth naturally by diminishing the ability of the first-born embryos to compete unfairly for the available water.

4. Some implications for hail suppression

One way of attempting to suppress hail is to try to emulate nature by generating further competing embryos in the parts of the updraft containing abundant supercooled water just beneath the main region of growing hailstones. According to Browning and Foote (1976), this approach may be be possible in the case of supercells because it requires the generation of competing particles within the vault where the updraft is persistently too strong to give enough time for competing particles to develop. The situation appears to be better in an ordinary multicell storm provided one is able to take advantage of the time-evolving character of the individual updrafts and attempts to seed each cell prior to the development of the first. In this way one cannot only try to insure that the newly-introduced embryos are able to start depleting the cloud water before the development of the precipitation particles responsible for the first echo, but also, if the seeding is begun early enough, one can exploit the relatively slow updraft velocity during the earliest stage of growth of the daughter cloud so as to give more time for the competing embryos to become effective.

Much of the growth of the initial embryos in the Raymer storm was accomplished during ascent from cloud base to the first echo at the −12°C level. The level of formation of the first echo on this occasion was rather lower than usual for hailstorms; it can be as high as the −40°C level although perhaps a more typical value would be −20 to −30°C (Browning, 1975). If seeding is to be effective in slowing down the growth of such embryos and in producing many more of comparable size, it is probably necessary for it to cause the liquid water content to be substantially depleted by the $-20°C$ level. In some recent calculations Young (1975) has derived the seeding rate required to deplete (through glaciation) different proportions of the cloud water at different altitudes. He finds that the required seeding rate depends very sensitively on the updraft velocity. For a very weak updraft of 2 m s^{-1} at about 3 km MSL increasing upward linearly at 0.75 m s^{-1} km^{-1}, the seeding rate required to achieve 90% glaciation by the $-20°C$ level is of order 1 g min^{-1} km^{-2} of silver iodide; for an updraft of 4 m s^{-1} at 3 km increasing upward at 1.5 m s^{-1} km^{-1} the corresponding seeding rate is of the order of 30 g min^{-1} km^{-2}. For comparison, a typical seeding rate as used by NHRE is only 1 g min^{-1} km^{-2}, although this seeding rate could reasonably be increased by at least an order of magnitude. Of course, Young's calculations are highly simplified. No allowance is made for the decrease in concentration of silver iodide in the cloud due to turbulent diffusion. The assumed mode of nucleation may also be in error. Consequently these results must not be relied on in a highly quantitative way. However, they do suggest that a significant proportion of the supercooled water can be glaciated by the $-20°C$ level only if the seeding is applied at an early stage in the growth of each successive daughter cloud while the vertical velocities are still very weak. Updrafts often intensify quite rapidly in daughter clouds, however, and so it appears to be desirable to act quickly as soon as a growing daughter cloud is identified. As shown in Fig. 3, the developing daughter clouds are located many kilometers ahead (or to the right) of the mature updraft region: according to the above arguments this is where the seeding should be concentrated.

It is not clear for how long one should continue seeding a daughter cloud as it develops into the main updraft. One hopes that the early seeding will produce more and smaller embryos in the initial stages of growth so that they will compete among themselves for the available water when they later find themselves in the intensifying updraft. In some ways one would have liked to have been able to glaciate the mature updraft in order to be more certain of preventing significant further hailstone growth but, as Young has shown, there comes a stage in the intensification of the updraft beyond which reasonable seeding rates will no longer have any worthwhile effect. In any case there is good reason to avoid seeding the strong updraft very heavily since, according to Young, this might cause a reduction in surface rainfall. Seeding at moderate rates in a weak updraft on the other hand is more likely to have the opposite effect.

Seeding the regions of initial embryo development is the approach adopted by Schock (1971), Summers *et al.* (1972), and Abshaev and Kartsivadze (1973). Abshaev and Kartsivadze recommend seeding near the leading edge of the radar echo, up to 3 to 5 km ahead of it, as shown by the crosses in Fig. 4. The region denoted by the dots in Fig. 4, within the radar overhang, was the primary target of the seeding carried out by Sulakvelidze, Bibilashvili, and Lapcheva (1967), based upon the "accumulation zone" concept. The latter corresponds to the common practice of seeding in the mature updraft, which we now suggest is not the best procedure. Abshaev and Kartsivadze (1973) used radar to determine where to seed; however, since the initial embryo development is within daughter clouds before the "first echo" stage, it may sometimes be easier to identify the seeding locations visually (Summers *et al.*, 1972). Visibility from the ground is often obscured and so such observations are most reliably obtained from an aircraft.

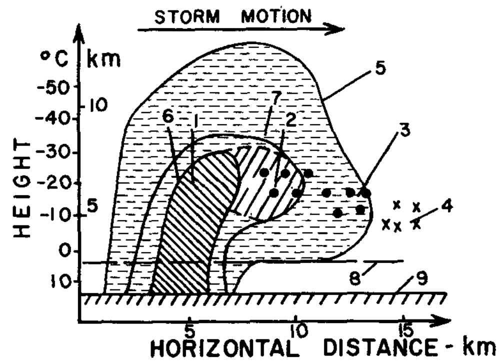

FIG. 4. Schematic diagram showing the preferred seeding location in an ordinary multicell hailstorm (after Abshaev and Kartsivadze, 1973). Features are identified by numbers as follows: (1) main hailshaft, (2) hail growth zone, (3) hail embryo formation zone, (4) seeding zone, (5) radar echo boundary, (6) zone of highest reflectivity, (7) boundary of region of fairly high reflectivity, (8) cloud base level, (9) surface level. The dots and crosses are discussed in the text.

It is important to keep in mind the limitations of the above discussion regarding the possibilities for hail suppression. What we have suggested on the basis of indirect inference is that the prospects for at least partial success in hail suppression seem rather more promising in ordinary multicell storms than in the archetypal supercell storms discussed by Browning and Foote (1976). We have also suggested a way of improving the chance of seeding having a beneficial effect. However, this suggestion is tentative; the observational evidence is scanty. Much more research is needed in the areas of the cloud dynamics, the hail trajectories, and the processes of natural hail growth (especially during the early stages of growth) before we can predict the outcome of different seeding procedures with any confidence. The possibility that a given seeding technique may have a different (sometimes adverse) effect on the precipitation in different kinds of storms makes it imperative that we avoid indiscriminate seeding and put more effort into developing a sounder, more quantitative, physical understanding.

Acknowledgments (*Parts I through V*). The authors are grateful to D. Atlas, G. B. Foote, C. A. Knight, W. C. Macklin, and J. D. Marwitz for helpful discussions and comments on the manuscripts and to all those within NHRE and collaborating agencies who contributed to the data collection and analysis.

REFERENCES

Abshaev, M. T. and A. I. Kartsivadze, 1973: Radar methods and equipment for hail suppression. *Proc. WMO/IAMAP Sci. Conf. Weather Modification,* WMO. No. 399, 343–350.

Auer, A. H., Jr. and J. D. Marwitz, 1968: Estimates of air and moisture flux into hailstorms on the High Plain. *J. Appl. Meteor.*, **7**, 196–198.

——, D. L. Veal and J. D. Marwitz, 1969: Updraft deterioration below cloud base. *Preprints, Sixth Conf. Severe Local Storms*, Chicago, Amer. Meteor. Soc., 16–19.

——, D. L. Veal and J. D. Marwitz, 1970: The identification of organized cloud base updrafts. *J. Rech. Atmos.*, **6**, 1–6.

Battan, L. J., 1953: Duration of convective radar cloud units. *Bull. Amer. Meteor. Soc.*, **34**, 227–228.

——, 1975: Doppler radar observations of a hailstorm. *J. Appl. Meteor.*, **14**, 98–108.

Browning, K. A., 1962: Cellular structure of convective storms. *Meteor. Mag.*, **91**, 341–350.

——, 1975: The structure and mechanism of hailstorms. A review paper presented at the NHRE Symposium, Sept. 1975. To be published.

——, and G. B. Foote, 1976: Airflow and hail growth in supercell storms and some implications for hail suppression. *Quart. J. Roy. Meteor. Soc.*, **102**. To be published in the July issue.

Byers, H. R. and R. R. Braham, Jr., 1949: *The Thunderstorm.* U. S. Gov't. Printing Office, Washington, D. C., 287 pp.

Cannon, T. W., 1974: A camera for photography of atmospheric particles from aircraft. *Rev. Sci. Instrum.*, **45**, 1448–1455.

Changnon, S. A., Jr., 1970: Hailstreaks. *J. Atmos. Sci.*, **27**, 109–125.

Chisholm, A. J. and J. H. Renick, 1972: The kinematics of multicell and supercell Alberta hailstorms. Alberta Hail Studies 1972, Research Council of Alberta Hail Studies Report No. 72-2, 24–31.

Danielsen, E. F., R. Bleck and D. A. Morris, 1972: Hail growth by stochastic collection in a cumulus model. *J. Atmos. Sci.*, **29**, 135–155.

Dennis, A. S., C. A. Schock and A. Koscielski, 1970: Characteristics of hailstorms of Western South Dakota. *J. Appl. Meteor.*, **9**, 127–135.

Dye, J. E., C. A. Knight, V. Toutenhoofd and T. W. Cannon, 1974: The mechanism of precipitation formation in northeastern Colorado cumulus, III. Coordinated microphysical and radar observations and summary. *J. Atmos. Sci.*, **8**, 2152–2159.

Goyer, G. G., W. E. Howell, V. J. Schaefer, R. A. Schleusener and P. Squires, 1966: Project Hailswath. *Bull. Amer. Meteor. Soc.*, **47**, 805–809.

Ludlam, F. H., 1958: The hail problem. *Nubila,* **1**, 12–96.

——, 1963: Severe local storms: A review. *Meteor. Monog.*, **5**, No. 27, 1–30.

Marwitz, J. D., 1972a: The structure and motion of severe hailstorms, Part I. Supercell storms. *J. Appl. Meteor.*, **11**, 166–179.

——, 1972b: The structure and motion of severe hailstorms, Part II. Multicell storms. *J. Appl. Meteor.*, **11**, 180–188.

——, 1972c: The structure and motion of severe hailstorms, Part III. Severely sheared storms. *J. Appl. Meteor.*, **11**, 189–201.

Musil, D. J., 1970: Computer modeling of hailstone growth in feeder clouds. *J. Atmos. Sci.*, **27**, 474–482.

Renick, J. H., 1971: Radar reflectivity profiles of individual cells in a persistent multicellular Alberta hailstorm. *Preprints Seventh Conf. on Severe Local Storms*, Kansas City, Mo., Amer. Meteor. Soc., pp. 63–70.

Rosinski, J., 1966: Solid water-insoluble particles in hailstones and their geophysical significance. *J. Appl. Meteor.*, **5**, 481–492.

—— and T. C. Kerrigan, 1969: The role of aerosol particles in the formation of raindrops and hailstones in severe thunderstorms. *J. Atmos. Sci.*, **26**, 695–715; corrigendum, **27**, 178–179.

Schock, M. R., 1971: The North Dakota Pilot Project: 1971 work plans. Inst. of Atmos. Sci., South Dakota School of Mines & Technology, Rapid City, Report No. 71–8, 23 pp.

Sulakvelidze, G. K., N. Sh. Bibilashvili and V. F. Lapcheva, 1967: Formation of precipitation and modification of hail processes. Israel Program for Scientific Translations, Jerusalem, 208 pp.

Summers, P. W., G. K. Mather and D. S. Treddenick, 1972: The development and testing of an airborne droppable pyrotechnic flare system for seeding Alberta hailstorms. *J. Appl. Meteor.*, **11**, 695–703.

Young, K. C., 1975: Growth of the ice phase in strong cumulonimbus updrafts. *Pure and Applied Geophysics*, **113**, 1005–1017.

Zipser, E. J., 1969: The role of organized unsaturated convective downdrafts in the structure and rapid decay of an equatorial disturbance. *J. Appl. Meteor.*, **8**, 799–814.